Advances in Excimer Laser Technology for Sub-0.25-μm Lithography

PALASH DAS AND RICHARD L. SANDSTROM

Invited Paper

There are several lasers that can provide high-power radiation at deep-UV wavelengths. The only laser that has been successfully used in semiconductor manufacturing as a source for lithography is the excimer laser. Excimer lasers provide direct deep-UV light, are scalable in energy and power, and are capable of operating with narrow spectral widths. Also, by providing three wavelengths at 248, 193, and 157 nm, excimer lasers span three generations. They have large beams and a low degree of coherence. Their physics and chemistry are well understood. Thanks to major technical developments, these lasers have kept up with the ever-tightening specifications of the lithography industry. We will discuss what these specifications are and the advances that have been made in laser technology to meet these. We will also identify any possible future limitation in this technology. The success behind the microelectronics explosion is attributed to many factors. The excimer laser is one of them.

Keywords*—*ArF lasers, excimer lasers, F_2 lasers, KrF lasers, lithography.

I. Introduction—Lasers in Microlithography

Microlithography is a manufacturing process for highly precise microscopic two-dimensional (2-D) patterns in a photosensitive resist material. These patterns are replicas of a master pattern on a mask. The mask is illuminated by a light source and then imaged on a wafer, coated with photoresist, by a lens. At the end of the lithographic process, the resist is used to create a useful structure in the device that is being built such as trenches on silicon wafer or a metal network on silicon. These structures then form the foundation for memory and processor ICs that go into computers, cellular phones, PDAs, and games, to name a few—everything that makes our lives more productive and fun.

Traditional light source for lithography has been the Hg–Xe Arc lamp. Its i line and g line are used for lithography below 256 MB DRAM. Its emission centered on 248 nm has also been used, but available power at this wavelength is very low. On the other hand, excimer lasers, such as the KrF at 248 nm, the ArF at 193 nm, and the F_2 laser at 157 nm, are sources of high-power radiation. They have relatively narrow spectrum as compared to Hg–Xe lamps, that is, they are considered to be high brightness sources. They provide direct tunable high-power output at the deep UV (DUV) without complex wavelength conversion schemes, as is the case with solid-state lasers. Their physics permit efficient spectral narrowing limited only by the quality of the narrowing optics. They can be scaled in power and repetition rate. Table 1 summarizes what was required, what they have evolved to, and what we might expect over the next few years from excimer lasers for lithography. Based on what the authors have experienced this past decade, we believe that excimer lasers will meet the lithography requirements for 16-Gb DRAM and 10-GHz microprocessors in the next ten years!

Solid-state lasers are other possible light sources. One example is alexandrite lasers at 248 nm and the other is diode-pumped, frequency multiplied solid-state laser at 248 and 193 nm. One apparent advantage they have over excimer lasers is that the factory does not have to deal with F_2 gases. However, considering the early start by excimer lasers and the ever-increasing power requirements, it is just too late for solid-state lasers to be viable light sources for advanced lithography.

II. Excimer Lasers and the Lithography Process

A. Wafer Exposure

The wafer exposure process involves the following systems: laser, optics to illuminate a mask, the mask itself, projection lens to image the mask on a wafer, a wafer-positioning system to position a chip on the wafer to the image of the mask, and the wafer itself. The reader is referred to two excellent textbooks ([4] and [6]) for an in-depth descrip-

Manuscript received October 15, 2001; revised June 15, 2002.

The authors are with Cymer, Inc., San Diego, CA 92127 USA (e-mail: Pdas@cymer.com; Rsandstrom@cymer.com).

Digital Object Identifier 10.1109/JPROC.2002.803665

Table I
Excimer Laser Requirements

Laser Specification	Effect On Scanner Performance	Requirements in 1995	Requirements in 2002
Wavelength	Resolution	KrF at 248nm	KrF at 248nm ArF at 193nm F2 at 157nm, develop.
Linewidth	Resolution, depth of focus	0.8pm @248nm	0.4pm @248nm 0.4pm @193nm ?? @ 157nm
Wavelength Stability	Focus & Resolution	±0.15pm	±0.05pm, all
Power	Throughput	10W @248nm	30W @248nm 20W @193nm 40W @157nm
Repetition Rate	Throughput	1000Hz @248nm	4000Hz, all
Dose Stability	CD control	±0.8% @248nm	±0.3% , all
Pulse Duration	Fused Silica Life @193nm	No Requirement	>40ns @193nm
Gas Lifetime	Uptime	100M @248nm	200M @248nm 100M @193nm 100M @157nm
Lifetimes For Chamber Line Narrowing Laser Metrology	Cost-Of-Operation	 4B @248nm 5B @248nm 5B @248nm	 12B @248nm 15B @248nm 20B @248nm 5B @193nm 5B @193nm 5B @193nm 5B @157nm 5B @157nm 5B @157nm

tion about lithography and all the technologies that support this field. The web sites of the three key lithography toolmakers–ASML, Canon, and Nikon—also contain excellent information about steppers and scanners.

The mask defines the pattern that is projected onto the chip (technically, the structure on the wafer is a die that becomes a chip when the die is saved up and packaged). The substrate of the mask is about 150 mm × 150 mm × 6 mm fused silica blank on which the circuit pattern is deposited. The deposited material is usually chromium. Fused silica has good transmission at 248 and 193 nm. The presence of OH groups in fused silica severely limits 157-nm transmission. However, recently, the fused silica transmission at 157 nm was increased to nearly 80% by reducing its OH content and doping it with fluorine [1]. Now, it appears that fused silica masks could be used for all three excimer laser wavelengths.

The projection lens is a large compound lens made up of over 20 simple elements mounted in a rigid barrel. The large numbers of elements are required to correct optical aberrations to better than $\lambda/10$ over the exposure field. The lens produces the optical image of the mask, reduced by a factor of 4. A silicon wafer is exposed to this image, which is captured by the layer of photoresists. The image is eventually developed to leave the resist pattern on silicon. The lens at the KrF wavelength is not chromatically corrected as it is made of entirely one material: fused silica. The natural linewidth of the laser ($\sim$ 300 pm) is too broad for the image quality requirements, hence the narrow spectral width requirements from the excimer laser. Thus, for a lens of $NA = 0.6$, the full-width at half-maximum (FWHM) requirement is about 0.8 pm. At 193 nm, the projections lens requires some color correction. Otherwise, the laser linewidth requirements are much lower than what is practically possible. Thus, a combination of fused silica and CaF_2 is used with a great increase in lens costs. The situation for F_2 is still open, but very likely the material would be CaF_2 and a catadioptric lens would be used instead of the refractive lens for KrF and ArF. Therefore, line narrowing may not be required for F_2.

B. Stepper and Scanner

The wafer positioning system is probably the most precise mechanical system in existence. It positions the wafer, either 200 or 300 mm in diameter, under the lens to a precision of better than 20 nm. The motion of the wafer positioning system coupled with the exposure technique determines two classes of lithography systems—stepper and scanner.

The stepper system exposes one chip at a time, as shown in Fig. 1 The light source exposes the full mask that contains the chip information and the lens images the mask on to the chip. The exposure field of the lens matches the chip size, so is about 28 to 30 mm in diameter. The number of pulses the

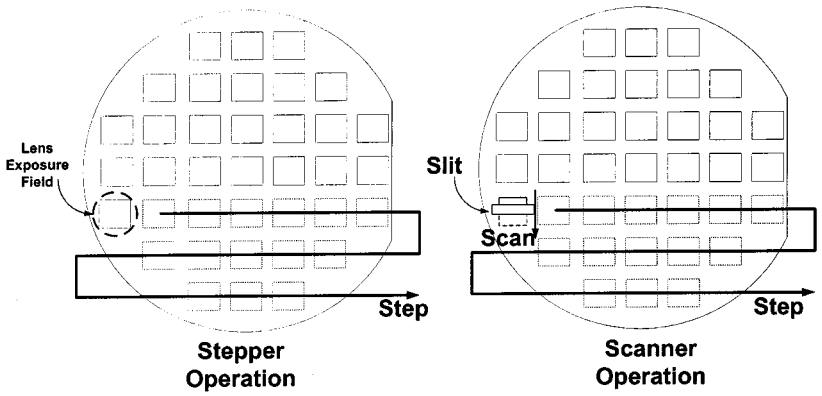

Fig. 1. Exposure of a wafer with a stepper and a scanner.

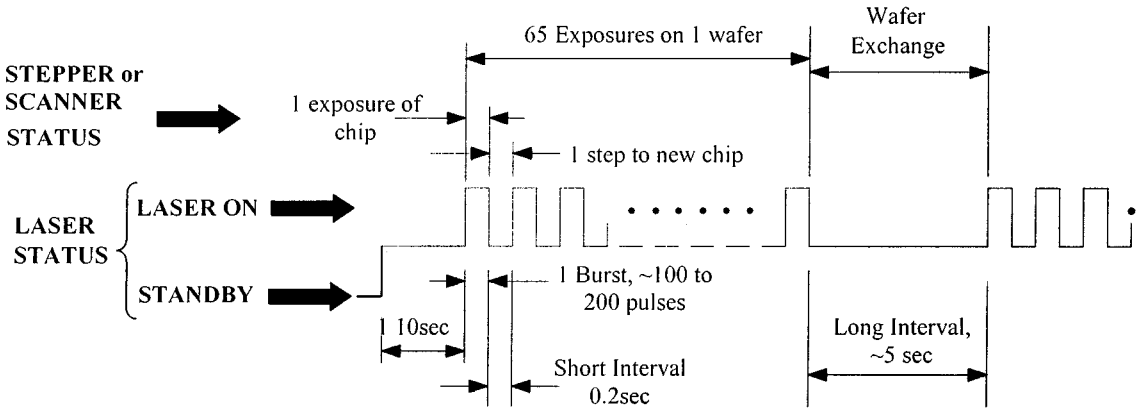

Fig. 2. Operation of an excimer laser with a stepper or a scanner.

laser fires on each chip is equal to the total energy required to expose the resist. After each chip, the wafer positioning system steps the wafer to next chip.

A scanner exposes the chip by "painting" a slit over the wafer (Fig. 1). After a chip is exposed, the wafer is stepped to the next chip and the exposure is repeated. This is done by scanning the mask and the wafer through the slit while the lens remains stationary. Slit height and width then determine the field size requirements of the lens. The slit height is matched to the smaller dimension of the chip ($\sim$ 25 mm) and the slit width is between 7–8 mm. Since only a smaller part of the chip is imaged, a smaller part of the lens is utilized. Therefore, the part of the lens with the least aberrations and best imaging is used. The process of scanning the chip increases the overall field size cost-effectively. As the requirements for lenses have tightened over the last five years [2], all lithography equipment manufacturers have now switched to scanner technology for their advanced tools despite the added mechanical complexity of scanning a wafer and mask during exposure.

The scan and step of a scanner and expose-and-step operation of a stepper impacts the operation of the laser. Excimer lasers operate in burst mode, meaning that they expose for few hundred pulses, and then wait for a longer period during wafer exchange (Fig. 2). Continuous operation is the preferred operating method of an excimer laser much like a lamp. Continuous operation permits stabilization of all laser-operating conditions, such as gas temperature and pressure. Based on the exposure conditions shown in Fig. 2, continuos operation implies a 50% waste of pulses. Laser manufacturers now live with burst mode operation despite the presence of significant transients in energy and beam pointing at the start of a burst. Fortunately, these transients are predictable and the laser's control software corrects for these transients [3]. Once the laser's controller learns the transient behavior of the laser, as seen in Fig. 3, the subsequent wafers are exposed correctly. In practice, the laser's software learns about the transient behavior prior to exposing wafers.

III. Advances in Excimer Lasers Specifications for Lithography

A. Introduction and History

The first excimer lasers for lithography exposure tools were introduced more than a decade ago. But it was only in 1997 that Hg i-line light sources at 365 nm were replaced with excimer lasers in volume manufacturing of semiconductor devices. The transition from Hg lamp light source technology to excimer technology is clearly illustrated in Fig. 4. As one can see, this Hg-to-excimer transition was driven by the need to make sub–0.25-μm features in semiconductor devices. Based on Rayleigh's criterion, one would think that the introduction of shorter wavelengths should have occurred much earlier, either in 1993 or 1995.

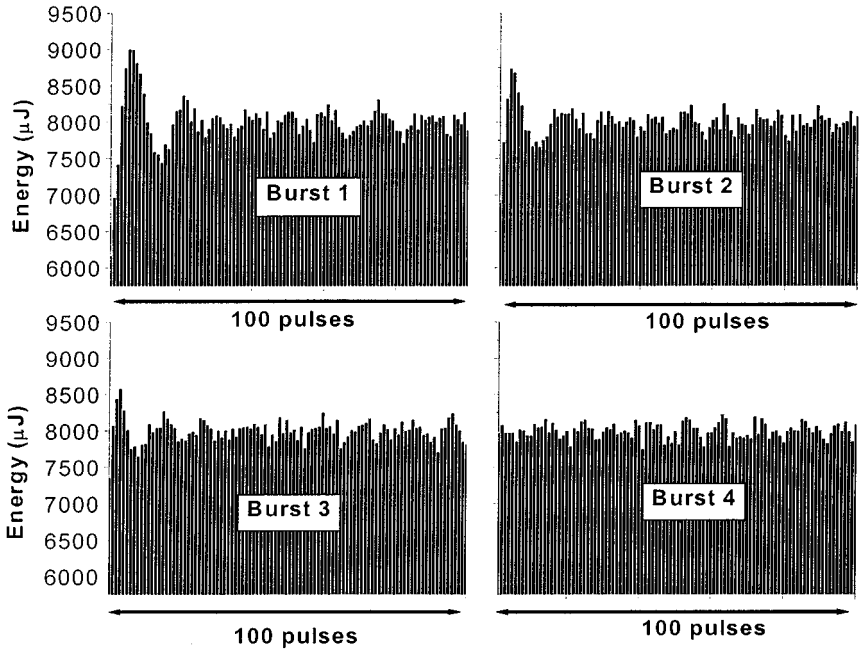

Fig. 3. Transients in energy during burst mode operation of an excimer laser for a stepper or scanner. The software learns the energy transients and, by the fourth burst, corrects for the transients. The software remembers these transient effects during subsequent exposures. The transients change when the operating conditions change, such as a time interval between bursts.

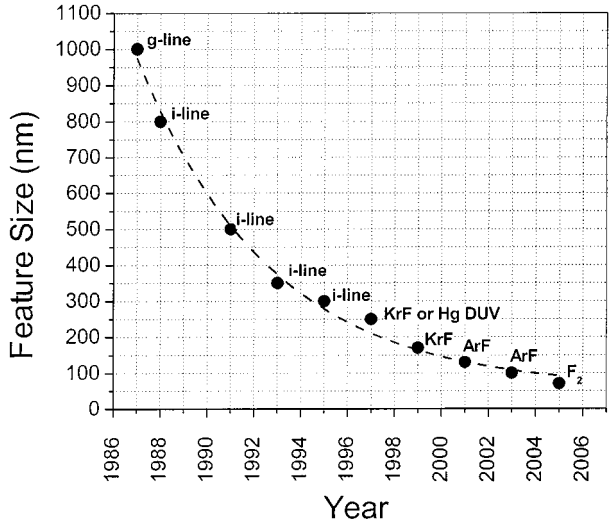

Fig. 4. The evolution of feature size on a wafer and the light sources used to achieve the feature size. The information has been gathered from numerous sources.

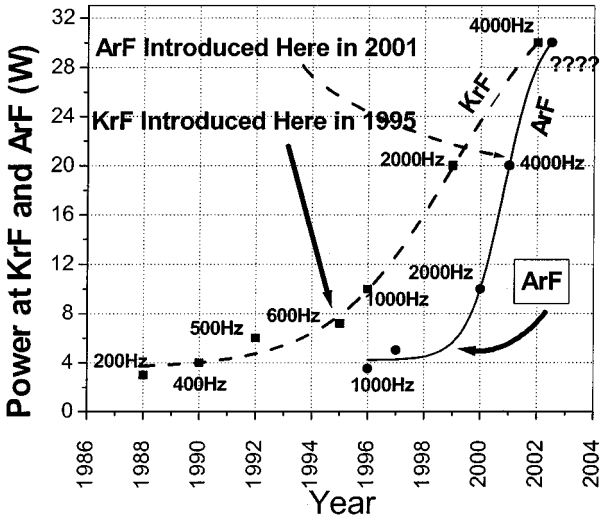

Fig. 5. The evolution of laser power and repetition rate for KrF and ArF excimer lasers for lithography. This graph is based on what the authors have observed over the past 15 years.

Rayleigh's criterion states that the resolution of an imaging lens with a numerical aperture NA is affected by the wavelength λ given in

$$R = k_1 * \frac{\lambda}{NA} \tag{1}$$

where k_1 is the dimensionless process k-factor. The larger the process k-factor, the easier it is to produce the chip, but at the expense of the resolution of the imaging lens.

KrF at 248 nm would have been a better source wavelength than the i-line at 365 nm in 1995 for 0.3 μm features or even in 1993 for 0.35-μm features. However, associated with each transition in wavelength are enormous technical issues related to photoresists and materials (primarily optical) at the new wavelength. Instead, two techniques were used to extend the i-line. One was to increase the NA of the lens from 0.4 to 0.6. The other was to decrease the process k factor from 0.8 to 0.5. By 1995, DUV-grade fused silica and 248-nm resists development were complete and the KrF laser became the mainstay of semiconductor manufacturing. Ironically, the issues that prevented the entry of KrF lasers would now extend its usability to beyond 0.18 μm. The entry feature size for ArF is 0.13 μm and that for F_2 is probably 0.07 or 0.05 μm.

The delayed entry of each excimer wavelength into the semiconductor manufacturing process has an enormous impact on both the present excimer wavelength and the new wavelength. Figs. 5 and 6 show how the delay in the introduction of excimer technology impacted the requirements

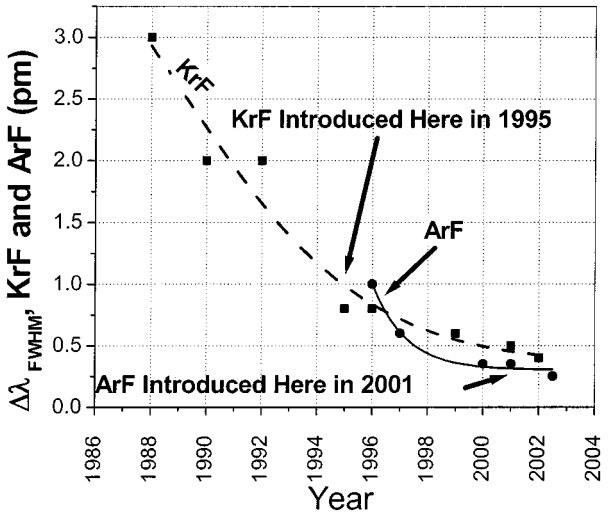

Fig. 6. The evolution of laser spectral linewidth for KrF and ArF excimer lasers for lithography. This graph is based on what the authors have observed over the past 15 years.

on KrF. Likewise, these figures show the impact on delayed entry of ArF on KrF and vice versa. Thus, in 1995, the laser's two critical parameters, power and linewidth, were significantly more stringent than in 1993. In the year 2002, the output of a KrF laser would be 30 W with linewidths of about 0.4 pm. Such power and linewidth requirements from KrF were not expected in the mid-1990s, and we had expected that KrF would end at 20 W and 2 kHz. The authors hesitate to guess where the entry point of F_2 would be due to frequent changes in technology roadmaps.

B. Power and Repetition Rate

The requirement for high power and repetition rate is determined by the throughput requirements of scanner. The scanner exposure time is given by

$$T_s = \frac{W+S}{V} \tag{2}$$

where

- T_s scanner exposure time for a chip;
- W chip width;
- S slit width;
- V scan speed for the chip.

For a given chip width, the slit width must be minimized and the scan speed must be maximized to reduce T_s. In general, the slit width is matched to the maximum wafer speed as follows:

$$S = V_m * \frac{n}{f} \tag{3}$$

where

- V_m maximum wafer scan speed;
- n minimum number of pulses to make the dose on wafer with the required dose stability—the dose is the integrated energy over n and dose stability is usually an indicator of how this dose varies from the target dose;
- f laser's repetition rate.

Advanced scanners are capable of scan speeds of 300 mm/s and are expected to reach 500 mm/s in the next few years. Therefore, to minimize S, the ratio n/f must be minimized. The number n cannot be very small due to the fact that a finite number of pulses are required to attain a specific dose at the wafer with a given dose stability. A typical number is 100 pulses to attain a dose stability of $\pm 0.25\%$. Slit widths of 7–8 mm are common. For a 7-mm slit width, a 300-mm/s scanner would require repetition rates of $\sim$ 4300 Hz.

Notice that the above analysis is independent of wavelength. Hence, if the exit point for KrF is 4 kHz, then the entry point for ArF is also at 4 kHz. This is no small task, considering that the first ArF lithography laser for R&D development, shipped in 1998, was only 1 kHz.

C. Spectral Linewidth

As stated by Rayleigh's criteria, the resolution of an imaging system could be improved by increasing its NA. In the mid-1990s, only fused silica was fully qualified as the suitable lens material at KrF wavelengths. Recently, however, UV-grade CaF_2 materials in sizes large enough for imaging lenses became available. For KrF, the lenses did not correct for chromatic aberration. The increase in NA severely narrowed the linewidth ($\Delta\lambda_{\mathrm{FWHM}}$) requirements, shown as follows [4]:

$$\Delta\lambda_{\mathrm{FWHM}} \approx \frac{(n-1)\lambda}{2f(\frac{dn}{d\lambda})(1+m)NA^2} \tag{4}$$

where

- n refractive index of the material;
- λ wavelength;
- $dn/d\lambda$ material dispersion;
- m lens magnification;
- f lens focal-length.

The equation predicts that, at $NA = 0.7$ and 0.8, at KrF wavelengths, the linewidth requirements would be 0.6 and 0.45 pm, in close agreement with what lens designers have required of KrF lasers. At 193 nm, due to the large increase in dispersion in fused silica, the same $NA = 0.7$ and 0.8 would require linewidths of 0.2 and 0.15 pm, respectively. Such narrow linewidths from excimer lasers were not practical in the mid-1990s when the technical approach for ArF lithography was formed. Hence, ArF lenses were chromatically corrected by using a combination of fused silica and CaF_2. However, the delay in availability of large lens quality CaF_2 by at least two years delayed the introduction of ArF, and KrF continued to be the laser of choice until recently.

D. Wavelength Stability

The penalty for high NA of a lens manifests itself in another way as well. The Rayleigh depth of focus (DOF) is related to the to the NA of the lens via the following equation:

$$\mathrm{DOF} = \pm 0.5\frac{\lambda}{(NA)^2} \tag{5}$$

Thus, for a $0.6NA$ lens at 248 nm, the DOF is about ± 0.35 μm, and for a 0.8 NA the DOF is only ± 0.2 μm. A change in wavelength induces a change in focus. This

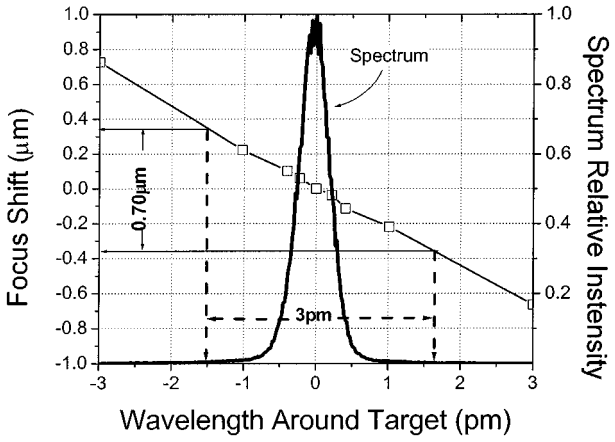

Fig. 7. Measurement of best focus as a function of wavelength and the shape of a KrF line.

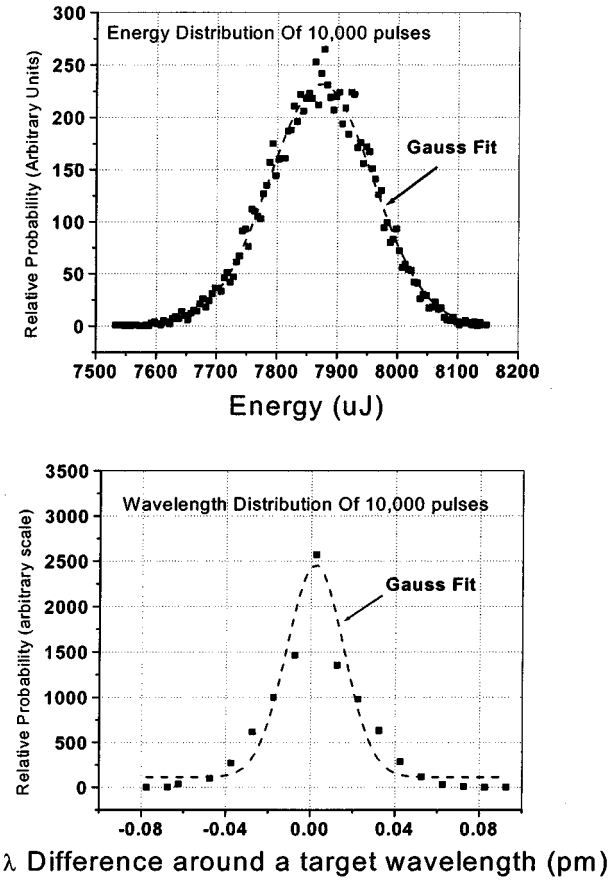

Fig. 8. The distribution of energy and wavelength (around the target wavelength) over 10 000 pulses for KrF laser.

is shown in Fig. 7 for a 0.6 NA lens at 248 nm. The permissible change in wavelength to maintain the focus of the lens is large, about 3 pm. However, the 3-pm range also restricts the spectral distribution of the laser line shape. If the laser contains significant energy ($> 5\%$) in the tails of its spectrum that extend beyond the acceptable wavelength range, the imaging properties of the lens deteriorates [5]. The spectral distribution encompasses all the energy from the laser within the DOF of the lens. However, during laser

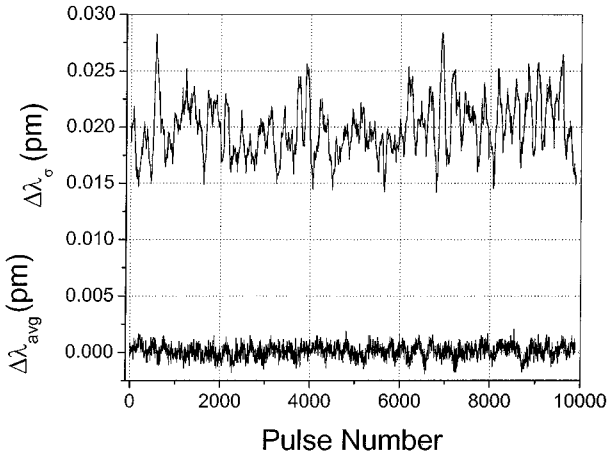

Fig. 9. The calculated wavelength stability for a KrF laser. Wavelength stability is characterized by two parameters. The first in wavelength standard deviation around mean ($\Delta\lambda_\sigma$) and the other is average wavelength around mean ($\Delta\lambda_{\text{avg}}$). The averaging is normally done over the number of exposed pulses for a chip, typically 100.

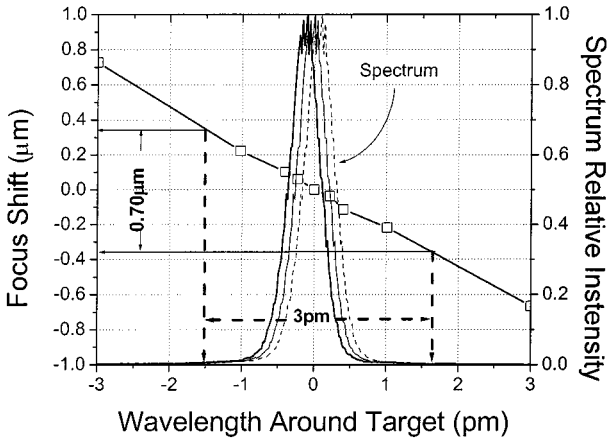

Fig. 10. The effect on a laser's spectral shape due to the laser's $\Delta\lambda_\sigma$ stability.

operation, stochastic processes that cause energy fluctuation also lead to a laser's wavelength fluctuation. As a result, the spectral distribution during exposure is actually an envelope due to the fluctuations. The effect of wavelength fluctuations on focus could be analyzed easily when one realizes that wavelength fluctuations are normally distributed just as energy fluctuations (Fig. 8). Thus, these wavelength fluctuations could be characterized in the same manner as energy fluctuations—as standard deviation around the mean ($\Delta\lambda_\sigma$) and as the deviation of an average number of pulses from the target ($\Delta\lambda_{\text{avg}}$). Fig. 9 shows $\Delta\lambda_\sigma$ and $\Delta\lambda_{\text{avg}}$ over 100 pulses of the aforementioned KrF laser. $\Delta\lambda_{\text{avg}}$ is close to target (i.e., near zero), but the magnitude of $\Delta\lambda_\sigma$ is not insignificant. During the exposure of the chip, the $\Delta\lambda_\sigma$ fluctuations tend to broaden the spectrum. This effect is shown in Fig. 10, which is Fig. 7 with the $3\Delta\lambda_\sigma$ fluctuation superimposed. The net result is that the specification of $\Delta\lambda_{FWHM}$ and $\Delta\lambda_\sigma$ goes together. Combined, they could cause a lens to defocus at the wafer especially for high NA lenses [5]. In the next section, we discuss how the operation

of lasers at high repetition rates tends to have dramatic effects on wavelength stability.

The impact of nonchromatic lenses with high NA is their sensitivity to pressure and temperature changes [6]. For the $0.6NA$ lens at 248 nm, 1 mm of Hg change in pressure results in a focus shift of 0.24 μm. Also, a 1 °C change in temperature induces a focus shift of 5 μm. This high sensitivity to temperature and pressure increases the precision to which the corrections need to be made. The shift in focus could be compensated for by a shift in laser wavelength. Since these environmental changes can occur during the exposure, a rapid change in wavelength is required, usually at the start of chip exposure. In other words, the laser's target wavelength must be changed and the laser must rapidly reach the target within few pulses (< 10 pulses). The specification of the laser that relates to how closely it can maintain its target wavelength during exposure is the average wavelength from the target ($\Delta\lambda_{\text{avg}}$). Since rapid pressure changes of a fraction of a millimeter of Hg can occur, the laser must respond to changes in wavelength of few tenths of a picometer (as high as 0.5 pm). In the next section, we describe how advanced excimer lasers have adopted new technologies to lock the wavelength to the target to within 0.005 pm.

E. Pulse Duration

Under exposure to ArF radiation [7], fused silica tends to densify, according to

$$\frac{\Delta\rho}{\rho} = \kappa \left(\frac{NI^2}{\tau}\right)^{0.6} \tag{6}$$

where

- ρ density of fused silica;
- $\Delta\rho$ increase in density;
- N number of pulses in million;
- I energy density in mJ/cm^2;
- κ sample-dependent constant;
- τ integral square pulse duration and is defined by

$$\tau = \left(\left(\int P(t)dt\right)^2\right) / \left(\int P(t)^2 dt\right)$$

where $P(t)$ is the time-dependent power of the pulse.

The refractive index of fused silica is affected by densification. After billions of pulses, the fused silica lens would seriously affect the image. Experience has shown that the magnitudes of κ can vary greatly depending on the fused silica supplier, meaning that the details of manufacturing fused silica is important. The other technique to increase lifetime is to reduce the intensity I by increasing repetition rate. The third technique is to stretch the pulse duration. Numerous fused silica manufacturers working in conjunction with International Sematech [8] are investigating the first solution. The laser manufacturers are investigating the other two. The validity of (6) has been questioned [8] at low energy densities (< 0.1 mJ/cm^2), comparable to the density experienced by a lens. Despite this ongoing debate on the effect of pulse duration, we expect that long pulse duration could soon become an ArF laser specification. Densification of fused silica appears to be restricted to ArF wavelengths.

F. Coherence

The requirements for narrower linewidth results in lower beam divergence. As a result, the spatial coherence of the beam improves. A simple relationship [9] between spatial coherence (C_s) and divergence (θ) is

$$\theta * C_s \approx 2 * \lambda. \tag{7}$$

With narrower linewidths, the coherence lengths have increased, and today, for a 0.4-pm KrF laser, the coherence length is about 1/10th the beam size in the short dimension and about 1/50th in the tall dimension. At the same time, narrower linewidth increases the temporal coherence of the beam. A simple relationship between temporal coherence (C_T) and linewidth is

$$C_T \approx \frac{\lambda^2}{\Delta\lambda}. \tag{8}$$

Do narrow linewidths make the excimer laser no longer an "incoherent" laser source? If the beam is no longer coherent, the lithography optics must correct for coherence effects. For the beam we referred to above, we could perform a simple calculation to answer this question. Based on the fact that the coherence length is 1/10th and 1/50th of the short and tall dimension, respectively, of the excimer beam, there are 10×50 (or 500) spatially coherent cells in the beam. The temporal coherence of the KrF laser with 0.5-pm linewidth is 123 mm. Combined, we may interpret this as 500 spatially coherent cells 123 mm in length exiting form the laser and then incident upon the chip during the laser pulse. Each of these 123-mm-long cells could cause interference effects, as they are fully spatially coherent. Since the pulse length of an excimer laser is about 25 ns, the number of temporally coherent cells during the pulse (product of speed of light and pulse length divided by temporal coherence length) is about 60.

Thus, the total numbers of cells that are incident on the chip are 500×60 or 30 000. All these contribute to interference effects or noise at the chip. We could then estimate speckle to be simply $1/\sqrt{N}$ where N is the total coherent cells or 30 000 or about 0.6%. This amount of speckle is not negligible considering the tight tolerance requirements of the features in present day semiconductor devices. This is the sad fact of life—narrow linewidths imply a coherent beam. These two properties go together, and the lithography optics must handle the coherent excimer beam [9].

In summary, we see that the requirements of excimer lasers have increased significantly since they were introduced for semiconductor R&D and then for volume production. The exponential growth in power requirements at all wavelengths, in combination with a massive drop in $\Delta\lambda_{\text{FWHM}}$ specification, is spurred by the drive for higher resolution features on wafers and higher wafer throughputs from scanners. In Section IV, we will describe the key technologies that comprise an excimer laser and what changes were required to make these lasers meet the challenging demands.

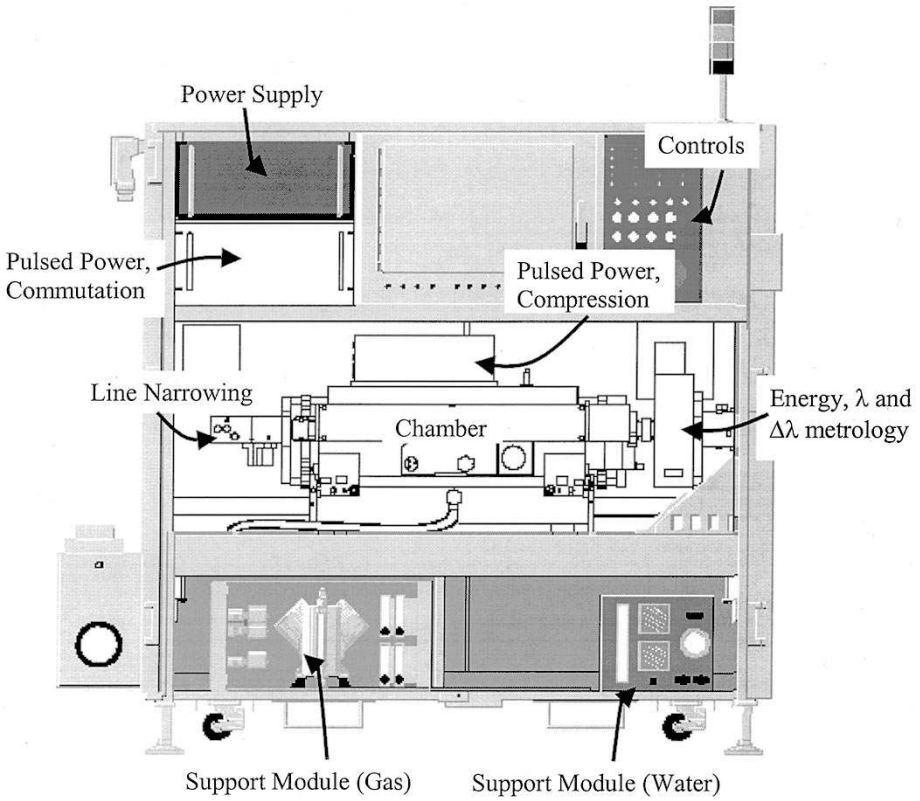

Fig. 11. The key modules of an excimer laser for lithography.

IV. Advances in Excimer Laser Technology

A. Laser Modules

The lithography excimer laser consists of the following major modules:

1) chamber;
2) pulsed power;
3) line narrowing;
4) energy, wavelength, and linewidth monitoring;
5) control;
6) support.

The control and the support modules have kept up with the advances in laser technology and will not be discussed here. Fig. 11 shows the layout of a commercial excimer laser for lithography. Typical dimensions for a laser at 2 kHz are about 1.7 m in length, 0.8 m wide, and about 2 m tall. Since these lasers occupy clean room space, the laser manufactures are sensitive to the laser's footprint. In the last seven years, as the laser's power increased threefold, the laser's footprint remained virtually unchanged.

B. Chamber

The discharge chamber is a pressure vessel designed to hold high pressure F_2 ($\sim 0.1\%$ of the total) gas in a buffer of krypton and neon. Typical operating pressures of excimer lasers range from 250 to 500 kPa, out of which 99% is neon for KrF and ArF and helium for F_2. The chambers are quite massive, usually greater than 100 kg. One would think that the chamber sizes have increased with output power. However, it appears that scientists and engineers have learned how to get more power from the same chamber. Thus, the same chamber that produced 2.5 W in 1988 produced 20 W in 1999!

Fig. 12 shows a cross section of the chamber. The construction materials of present day chambers are aluminum, nickel, and brass [10]. The only nonmetallic material that comes in contact with gas is 99.5% pure ceramic. The electrical discharge is initiated between the electrodes. The electrode shape and the gap between the electrodes determine the size and shape of the beam. Typical beam widths are 2–3 mm and heights range from 10 to 15 mm. It is advantageous to keep the beam size large. A large beam assures that the beam is multimode and hence spatially more incoherent than single-mode lasers. We will discuss the issue of beam coherence in the next section.

The energy that is deposited between the electrodes heats the gas adiabatically. This heating generates pressure waves originating at the electrodes that travel to the chamber walls and other structures. These structures could reflect the sound waves back to the electrode region. At a typical gas operating temperature of 45 °C, the speed of sound in neon is about 470 m/s. In 1 ms, the sound wave must travel 47 cm before it can reach the electrode region coincident with the next pulse. Considering the dimensions of the chamber shown in Fig. 12, the sound wave must have made a few reflections before it reached the electrode region 1 ms later. The reflected wave after 1 ms is weak. However, at 2 kHz, the sound wave must travel only 23.5 cm before it is coincident with the next pulse. Although the gas temperature determines the exact timing of the arrival waves, the dimension of the chamber and the lo-

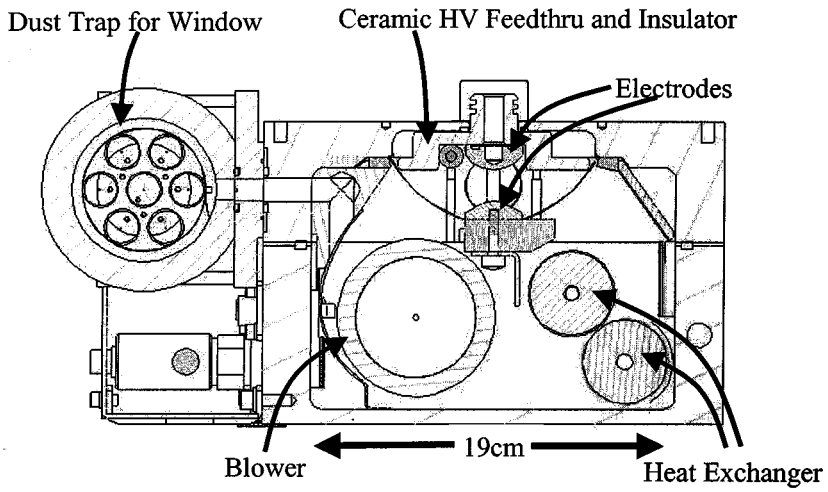

Fig. 12. The cross section of an excimer laser chamber.

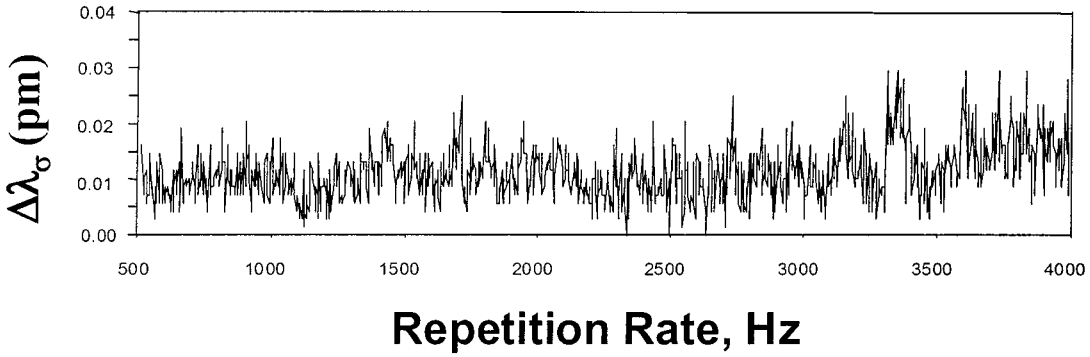

Fig. 13. The increase in wavelength stability $\Delta\lambda_\sigma$ as a function of repetition rate.

cation of structures within almost guarantees that some reflected sound wave is coincident with the next 2-kHz pulse. The situation is much worse at 4 kHz, since the sound wave must only travel less than 12 cm.

Additionally, during burst mode operation of the laser, typical during scanner exposure, the laser gas temperature changes over several degrees over a few milliseconds. These changing temperatures change the location of the coincident pressure waves from pulse to pulse within the discharge region. In turn, this affects the index of refraction of the discharge region, causing the laser beam to change direction every pulse. The line narrowing technology described below is sensitive to the angle of the incident beam. A change in angle of the incident beam in the narrowing module would induce a change in wavelength. Fig. 13 shows this wavelength variation in from a chamber (with a line narrowing module) at a fixed temperature ($\sim 45\,^{\circ}\mathrm{C}$) as a function of repetition rate. This variation results in a loss of control of the target wavelength and also causes an effective broadening of the spectrum, as discussed in the previous section. This problem manifests itself at a high repetition rate and worsens as the repetition rate increases. Also, depending on the gas temperature, the repetition rate, and the location of structures near the discharge, there is some resonant repetition rates where stability is much worse.

The effect of these pressure waves can also be seen in a laser's energy stability, beam pointing stability, beam uniformity, and linewidth stability. A proper choice in temperature and spacing between the discharge and structures may delay the pressure waves for a particular repetition rate but not for another. Since excimer lasers in lithography applications do not operate at a fixed repetition rate, temperature optimization is hardly a solution. The other impractical solution is to increase the distance of all support structures around the discharge—which would lead to a larger chamber for every increase in repetition rate. This implies that, at 4 kHz, the cross section of the chamber would be four times larger! Previous attempts in mitigation of such waves utilized "sponge-like" materials in the chamber that absorbed the pressure waves—but at the expense of severely contaminating the laser gas.

While the presence of these pressure waves does not bode well for high-repetition-rate excimer lasers for the future, very innovative and practical techniques have been invented by a group of scientists [11]. They introduced several reflecting structures in the chamber shown in Fig. 12 such that the reflected waves would be directed away from the discharge region. The reflecting structures, made from F_2 compatible metals, were designed to scatter the pressure waves. The effect of these so-called "baffles" is shown in Fig. 14.

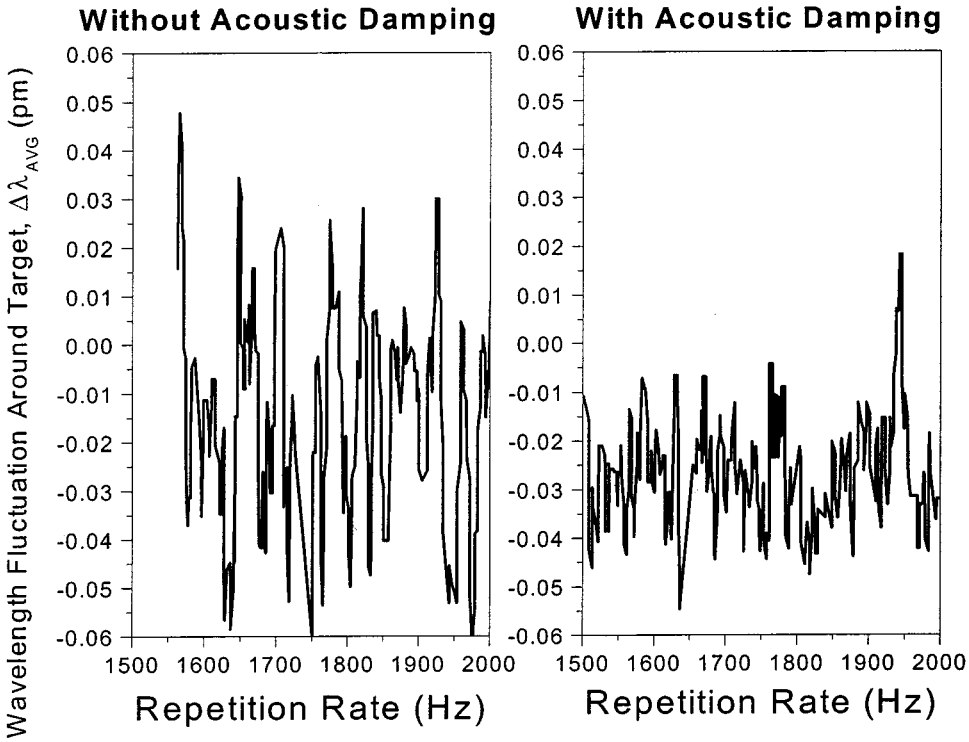

Fig. 14. The improvement in a laser's wavelength fluctuation (deviation from target wavelength) at 2000 Hz when acoustic damping is introduced in a chamber. The fluctuations reduce by a factor of about 3.

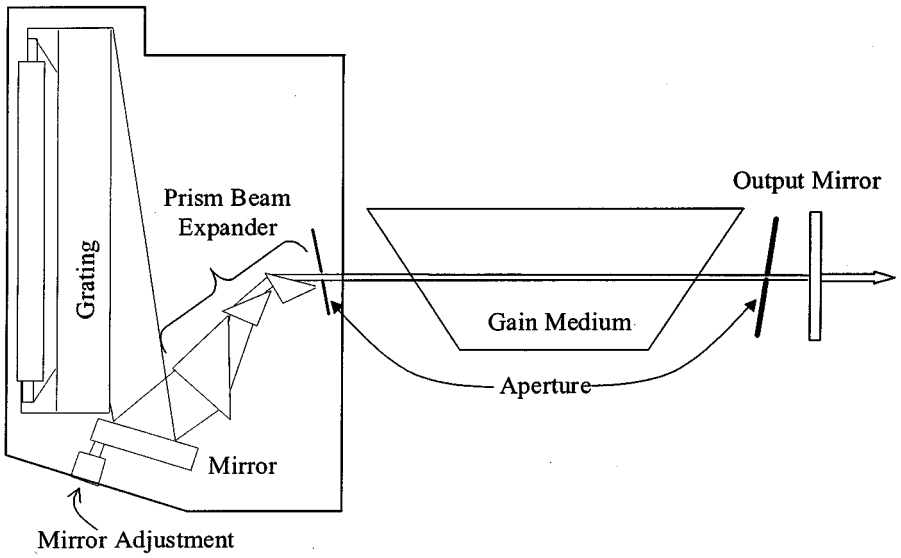

Fig. 15. The line-narrowing module of an excimer laser configured to operate with a chamber and output mirror.

These "baffles" reduce the wavelength variation by a factor of three for most repetition rates.

As the lithography industry continues to strive for higher scanner throughput via higher repetition rates, the excimer laser designers would face great technical hurdles related to the presence of pressure waves. Probably, other innovative ways must be investigated to increase scanner throughput.

C. Line Narrowing

The most effective line narrowing technique, implemented on nearly all lithography lasers is shown in Fig. 15 This technique utilizes a highly dispersive grating in the so-called Littrow configuration. In this configuration, that angle of incidence of the grating equals the angle of diffraction. Due to the dispersive nature of the grating, the linewidth is proportional to the divergence of the beam incident on the grating. Thus, the beam incident on the grating is magnified usually by a factor of 25–30 to fill the width of the grating. Prisms are used for beam expansion as they maintain the beam wavefront during expansion. Due to the fact that the beam attendue (product of beam divergence and beam dimension) is constant, the large beam reduces the divergence, which then re-

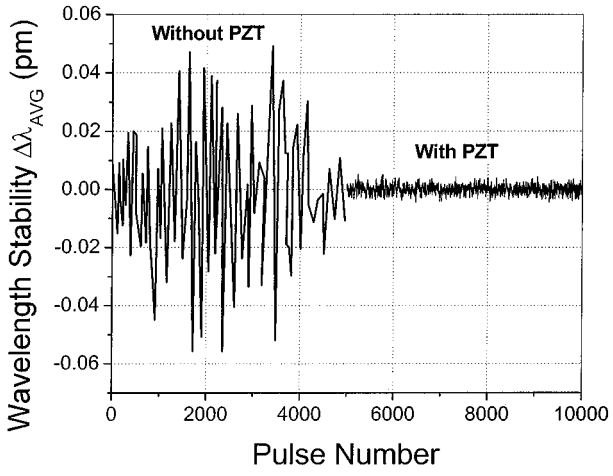

Fig. 16. Wavelength stability ($\Delta\lambda_{\mathrm{avg}}$) when the wavelength is adjusted to compensate for any deviation from the target using a fast adjustment based on PZT technology.

duces the linewidth of the laser. The beam divergence is also limited by the presence of apertures in the line-narrowing module and near the output mirror. These apertures effectively define the number of transverse modes or the divergence of the beam. The combination of high magnification, large gratings, and narrow apertures could be used in the future to meet the linewidth requirements. We expect that this technology could be extended to the 0.2-pm range.

Since the beam expansion prisms are made out of CaF_2 and the grating is reflective, this line narrowing technology is applicable to all three generations of excimer lasers—KrF, ArF, and F_2.

The angle of the beam incident on the grating determines the wavelength of the laser. Thus, adjusting this angle makes the wavelength adjustment of the laser. In practice, the mirror shown in Fig. 15 is adjusted to change the wavelength because it is less massive than the grating. Until recently, simple linear stepper motors were used to accomplish small wavelength changes. Typically, the minimum change in wavelength that could be accomplished was 0.1 pm over a period of 10 ms. This means that at 4000 Hz the response to change 0.1 pm would take about 40 pulses, which is nearly half the number used to expose a chip. Also, 0.1 pm corresponds to nearly 20%–30% of the laser's linewidth and hence is unacceptable. Recent advances made [12] in wavelength control technology have significantly reduced the minimum wavelength change to about 0.01 pm over a period of only 1 ms or 4 pulses at 4000 Hz. The mirror movement is now done by via a PZT driven adjustment. The rapid response of the PZT permits tighter control of the laser's wavelength stability as shown in Fig. 16. Also, the use of PZT permits rapid changes in wavelength to maintain the focus of the lens during the exposure of the chip. Thus, active adjustment of lens focus, due to pressure or temperature changes in the lens, might now be feasible.

D. Wavelength and Linewidth Metrology

Associated with tight wavelength stability to maintain focus of the lens is the requirement to the measure wavelength accurately and quickly (that is, every pulse). In 1995, the precision of wavelength measurements of ± 0.15 pm was adequate. Now, wavelengths must be measured to a precision of ± 0.01 pm, consistent with maintaining wavelength stability to within < 0.05 pm. In addition, the metrology must be capable of measuring linewidths from 0.8 pm in 1995 to 0.4 pm today. The fundamental metrology to perform these measurements has not changed since 1995. Fig. 17 shows the layout of the metrology tool integrated in the laser. Today such tools can measure wavelengths and linewidths at 4000 Hz more precisely than in 1995, without any significant change in its size.

The grating and the etalon are used to make an approximate and an accurate measurement of wavelength, respectively. The output from the grating is imaged on a 1024-element silicon photodiode array (PDA) as shown in Fig. 18. The fringe pattern of the etalon is imaged on one side of the grating on the PDA. The central fringe from the etalon is blocked intentionally so that it does not overlap with the grating signal.

The approximate wavelength is calculated straight from the grating equation

$$2d\sin\theta = m\lambda \tag{8}$$

where:

- d grating groove density;
- θ angle of incidence on the grating;
- m order of diffraction.

By selecting d and m appropriately, the knowledge of the angle is sufficient to provide the wavelength. The angle is measured from its position on the PDA. In practice, the PDA is calibrated with a known wavelength that encompasses all the constants of the grating and imaging optics. This equation only gives an approximate wavelength that is determined by the focal length of the lens and the location of the grating signal on the PDA with respect to the wavelength used for calibrating the PDA. In practice, it is adjusted to be within one free spectral range (FSR) of the etalon. This means that the grating computes the wavelength to within ± 5 pm.

The knowledge of the approximate wavelength coupled with the inner and outer fringe diameter of an etalon fringe is used to calculate the exact wavelength from

$$\lambda_1 = \lambda_0 + C_d(D_1^2 - D_0^2) + N * \mathrm{FSR} \tag{9}$$

where:

- D_0 and D_1 defined in Fig. 18;
- λ_1 wavelength corresponding to D_1;
- λ_0 caliberation wavelength;
- C_d calibration constant depending on the optics of the setup;
- FSR FSR of the etalon;
- N integer, $= 0, \pm 1, \pm 2, \pm 3$.

The magnitudes of λ_0, C_d, and the FSR are predetermined and saved by the tool's controller. The value of N is selected such that

$$|\lambda_1 - \lambda_g| \leq \frac{1}{2}\mathrm{FSR} \tag{10}$$

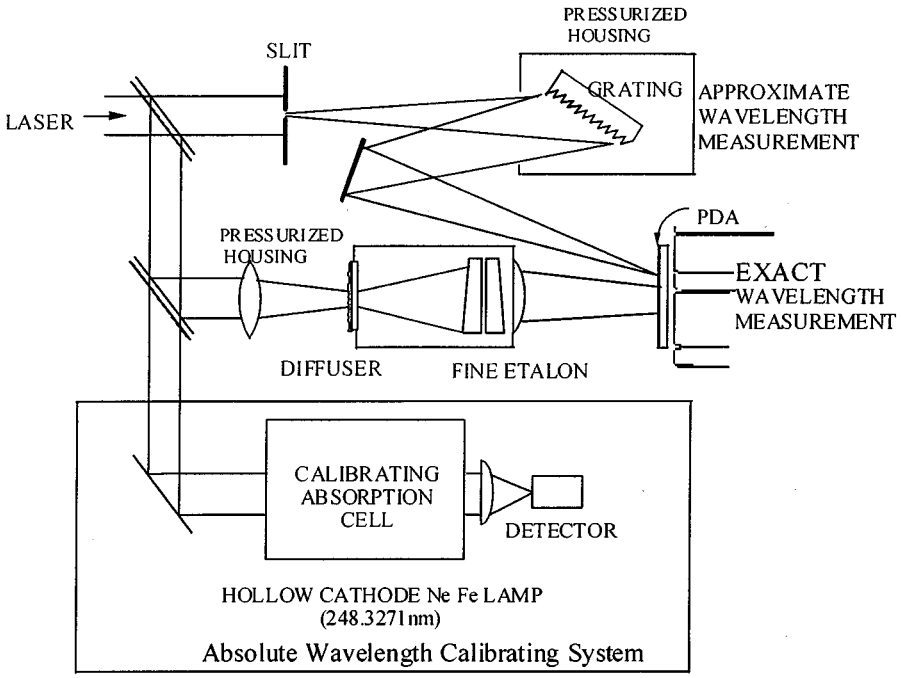

Fig. 17. The optical layout of a wavelength and spectral linewidth metrology tool.

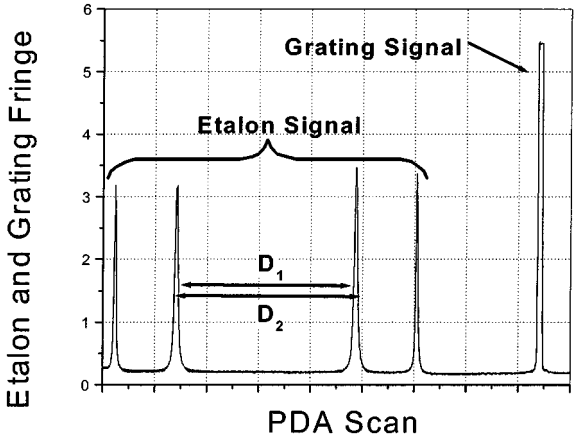

Fig. 18. The signals from the PDA of the metrology tool. The central etalon fringe is blocked.

where λ_g is the approximate wavelength calculated by the grating.

Similarly, λ_2 is calculated from D_2. The final wavelength is the average of λ_1 and λ_2

$$\lambda = \frac{\lambda_1 + \lambda_2}{2}. \tag{11}$$

Due to the laser's linewidth, each fringe is broadened. The laser's linewidth at full width at half maximum is calculated from

$$\Delta\lambda = \frac{\lambda_1 - \lambda_2}{2}. \tag{12}$$

Due to the finite finesse of the etalon, its FSR/finesse ratio limits the resolution of the etalon. Typically, the resolution is between 0.4–0.8 pm. This finite resolution broadens the measured linewidth in (12). The common practice to extract the correct linewidth is subtracting a fixed correction factor from (12).

As the linewidths continue to decrease with each generation of laser, practical techniques to extract linewidth must be refined. An innovative approach [13] uses a double-pass etalon to improve the etalon's resolution to measure linewidth.

The metrology for KrF and ArF is similar. For F_2 lasers, practical metrology that fits in a laser must be invented. If F_2 lasers are operated at their natural linewidth, the metrology may be simpler than if they are operated as line-narrowed lasers.

All metrology tools need periodic calibration to compensate for drifts in the optics of the tool. Fortunately, atomic reference standards exist for all the three wavelengths, and laser manufacturers have integrated these standards into the metrology tools. For KrF, the standard is an atomic iron line at 248.3271 nm (wavelength at STP conditions). For ArF, the standard is an atomic platinum line at 193.4369 nm (vacuum wavelength). For F_2, the standard is D_2 at 157.531 nm.

E. Pulsed Power

Excimer lasers require their input energies to be switched in very short times, typically 100 ns. Thus, for a typical excimer laser for lithography, at 5 J/p, the peak power into the laser is 50 MW. This may appear to be trivial until one considers the repetition rate ($\gg$ 1000 Hz) and lifetime requirements (switch life of $\gg$ 1 B pulses). High-voltage switched circuits such as those driven by thyratrons have worked well for excimer lasers in other industries—such as in medical. For lithography, the switching must be precise and reliable. The precision of input switched energy must be within 0.1%–0.2% and the reliability of the switching must be 100%. By 1995, it was realized that conventional

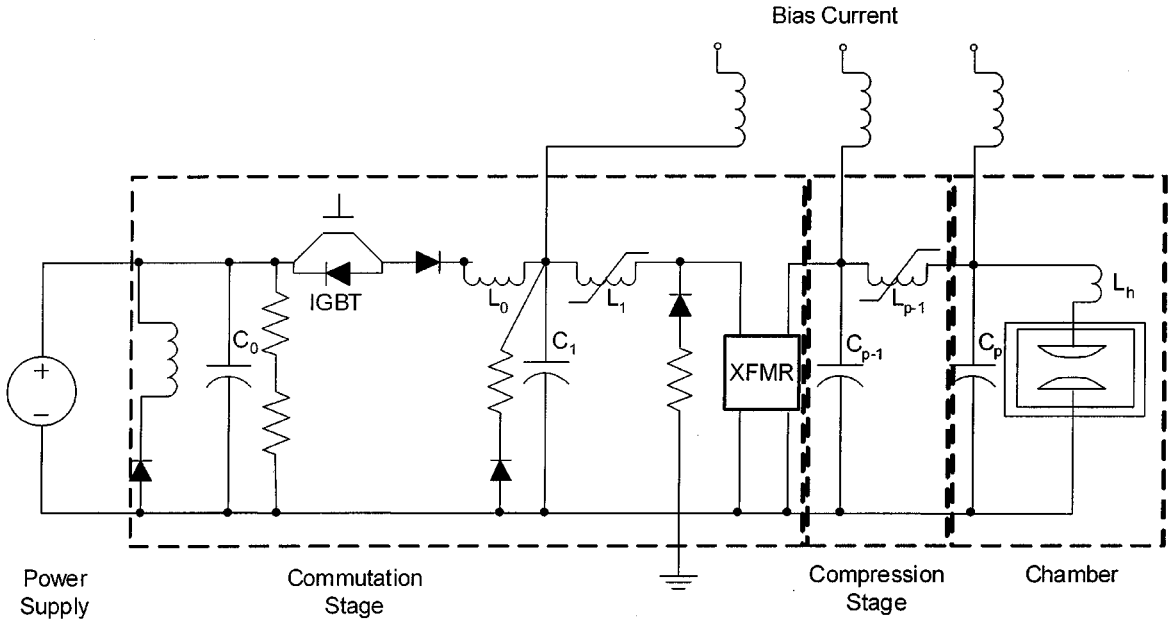

Fig. 19. A solid-state switched pulsed power circuit capable of operating at 4000 Hz. The primary switch is an IGBT, and the secondary switches are saturable magnetics.

switching with a high-voltage switch, such as thyratron, was not appropriate for this industry [14]. Thyratrons were unpredictable (high missed pulses) and limited in lifetime. Instead, solid-state switching, using a combination of solid-state switches, magnetic switches, and fast pulse transformers, was adapted. This proved to be worthwhile, as this same technology that switched lasers at 1 kHz would now be carried forward to all generations of excimer lasers.

Fig. 19 is a schematic of a solid-state switched circuit used in a 4000-Hz excimer laser [15]. The power supply charges the capacitor C_0 to within 0.1%. Typical voltages are less than 1000 V. Thus, a precision of 0.1% corresponds to 1 V. Typical values of dE/dV of these lasers are about 50 μJ/V. For an output energy of 5000 μJ per pulse, this corresponds to 1% of the energy. If the laser must achieve a dose stability of 0.3%, the precision of the supply cannot be greater than 0.1%.

When the insulated-gate bipolar transistor (IGBT) commutes, the energy is transferred to C_1. The inductor L_0 is in series with the switch to temporarily limit the current through the IGBT while it changes states from open to close. Typically, the transfer time between C_0 and C_1 is 5 μs. The saturable inductor L_1 holds off voltage on capacitor until it saturates, allowing the transfer of energy from C_1 through a step-up transformer to a C_{p-1} capacitor in a transfer time of about 500–550 ns. The transformer efficiently transfers the 1000-V, 20 000-A, 500-ns pulse to a 23 000-V, 860-A, 550-ns pulse that is stored in C_{p-1}. The saturable inductor L_{p-1} holds off the voltage on the C_{p-1} capacitor bank for approximately 500 ns and then allows the charge on C_{p-1} to flow onto the laser's capacitor C_p in about 100 ns. As the capacitors C_p get charged, the voltage across the electrodes increases until gas breakdown between the electrodes occurs. The discharge lasts about 50 ns during which the laser pulse occurs.

The excimer laser manufacturers have lived with the increased complexity of a solid-state switched pulsed power. This is because the switches have the capability of recovering residual energy in the circuits that are not dissipated in the discharge so that the subsequent pulse requires less input energy [14]. Today, solid-state switching and chamber developments proceed together. The long-term reliability of a lithography laser is as much dependent on the chamber as it is on its pulsed power.

F. Pulse Stretching

Previous investigations on long pulses from broadband ArF lasers have been sporadic [16], with the conclusion that a practical long-pulse ArF laser was not feasible. Recently, howere, a simple modification to the circuit shown in Fig. 20 was proposed [16]. The simplicity of the technique makes it an attractive technology for stretching ArF pulses. The other technique, already demonstrated in micro-machining applications with ArF lasers, involves a simple optical delay line. Both of these techniques could be commercialized if long pulses are indeed deemed necessary.

In the pulsed power technique, the capacitor C_p in Fig. 19 is replaced with two capacitors C_{p1} and C_{p2}, with a saturable inductor L_s in between. The compression module in Fig. 19 charges C_{p1}. The saturable inductor prevents C_{p2} from being charged until C_{p1} reaches a voltage close to twice the laser's discharge voltage. Once L_s saturates, charge is transferred to C_{p2} until the discharge breaks down. By adjusting the relative magnitudes of C_{p1} and C_{p2}, two closely spaced pulses are generated—one driven by C_{p2} and then the next by C_{p1}. Fig. 21 shows the stretched pulse and compares that with a normal ArF pulse.

Due to discharge stability issues, ArF pulses are inherently short ($\sim$ 20–25 ns). The penalty for a long pulse is a degradation of pulse stability by as much as 50%. On the other

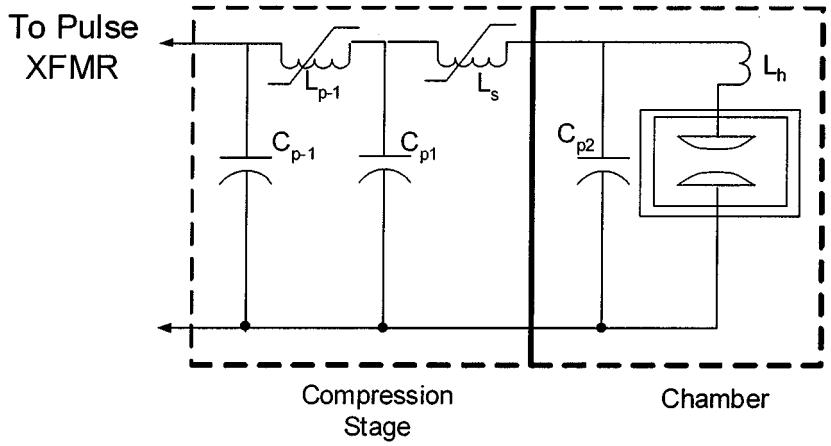

Fig. 20. A modification to the solid-state switched pulsed power of Fig. 19 where an extra stage of compression is introduced near the chamber. This extends the current pulse to the chamber, resulting in a longer optical pulse.

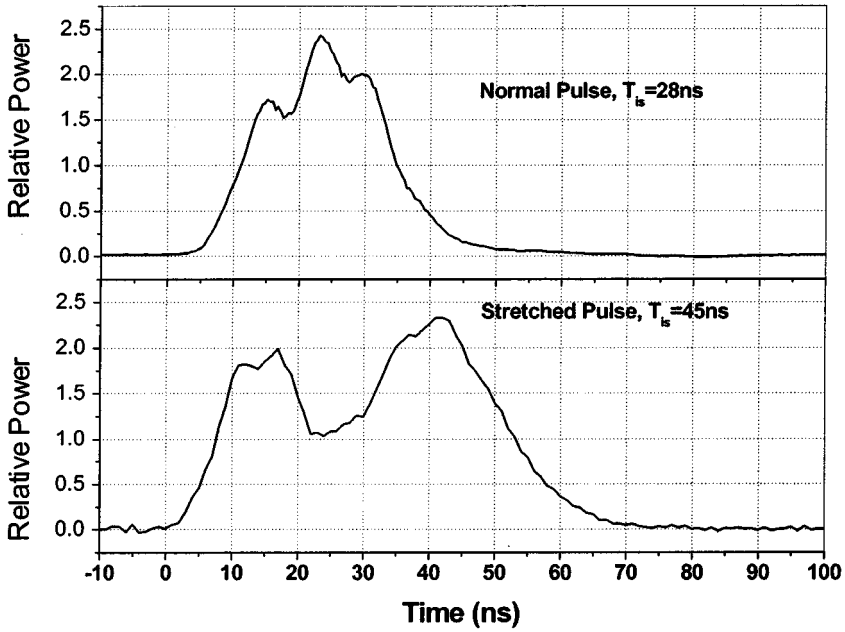

Fig. 21. A comparison of pulse shapes using the pulsed power in Figs. 19 and 20, respectively.

hand, the optical delay line involves multiple mirrors, and the total loss in power in such a configuration could be as high as 30%–40%.

G. Module Reliability and Lifetimes

When excimer lasers were introduced for volume production, their reliability was a significant concern. Various cost-of-operation scenarios were created that potrayed excimer lasers to be the cost center of the lithography process. The cost of operation is governed by three major components in the laser—chamber, line-narrowing module, and metrology module. The chamber's efficiency degrades as a function of lifetime measured in pulses. This is due to erosion of its electrodes. As a result, its operating voltage increases until the operating voltage reaches a maximum. The line-narrowing module's grating reflectivity degrades with lifetime, which makes the module unusable. The metrology tool's etalons and internal optics degrade due to coating damage until they cannot measure linewidth correctly. In all cases, end of life is gradual as a function of pulses. Thus, the end of life of the module can be predicted and that module replaced before the laser becomes inoperable. Today, most excimer lasers in a production environment have an uptime of 99.8%, which means the laser operates nearly all the time.

The laser manufacturers have combined good physics and engineering in making remarkable strides in lifetime. Fig. 22 shows a comparison of chamber lifetime in 1996 to that of today. This is remarkable considering that the present-day 20-W chamber is slightly smaller in size compared to the one in 1996. Similarly, the optical module lifetimes have improved fivefold by a combination of durable coatings and materials, understanding the damage mechanisms that limit coating lifetime, and by systematic studies of interaction of matter with DUV light. Initial lifetime estimates of ArF were of concern, but rapid strides have been made and, by year

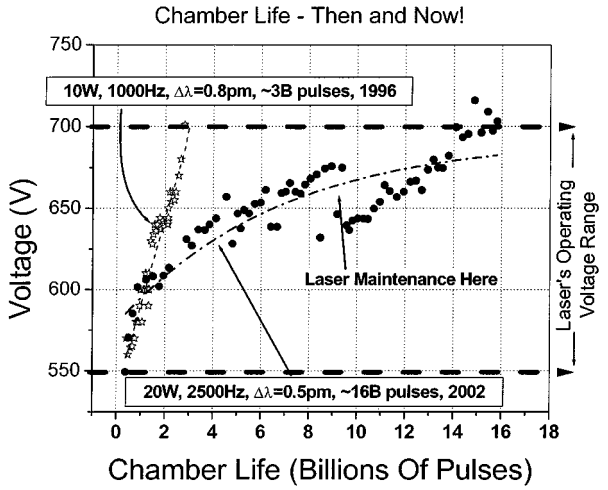

Fig. 22. The increase in the chamber's operating voltage as a function of the number pulses on the chamber. An increase in voltage indicates a decrease in laser efficiency. Beyond the laser's operating range, the output stability of the laser suffers, making the chamber unusable.

2003, the lifetimes would be comparable to KrF. F_2 is expected to match ArF.

H. Limitations in Excimer Technology for Future Requirements

An examination of technology roadmaps, such as the one published by the International Technology Roadmap for Semiconductors (ITRS), indicates that the power requirements from excimer lasers are expected to increase dramatically to match the throughput requirements of scanners. Thus, for ArF, the output power would be 40 W in 2003 and 60 W by 2005, as compared to 20 W today. Likewise, the linewidths are expected to decrease with shrinking feature size, to about 0.25 pm in 2003 compared with 0.4 pm today. Until recently, power increases have been handled by increasing the repetition rate of the lasers while keeping the energy same. However, this has resulted in increasing blower power to move the gas between the electrodes in the chamber. Given that blower power increases as the cube of the laser power everything else being held constant [17], a 40-W ArF laser would consume 28 000 W ($\sim$ 37 hp) of power compared to present-day consumption of 3500 W ($\sim$ 4.6 hp) for a 20-W laser. Likewise, these increasing power requirements severely stress the thermal capacity of line–narrowing technology.

The authors believe that the time has come to consider a major shift in laser architecture to achieve higher powers—freeze repetition rates and increase energy. A single chamber laser with associated line narrowing must be abandoned. Instead, an increase in energy is achieved by using a master-oscillator power amplifier (MOPA) configuration. A low-power, high-performance laser produces the required low linewidth at low energy (master oscillator) and a high-gain amplifier (power amplifier) boosts the output power to the required levels. The so-called MOPA architecture has shown extremely promising results and has been discussed in detail by one of the authors [17]. With this shift in laser architecture, the authors believe that excimer technology can continue to support the aggressive technology roadmaps of the semiconductor industry.

V. Summary

In this paper, we attempt to inform the reader that much has happened since excimer lasers became the light source for lithography. Today, excimer laser manufacturers are rapidly advancing the state of the technology at all three wavelengths −248, 193, and 157 nm. In the foreseeable future, we see that the power requirements could be met. However, we may have to rethink the scaling laws based purely on repetition rates. Instead, the authors propose a new MOPA architecture where power is scaled by increasing energy but freezing repetition rate.

Acknowledgment

The storage capacity of DRAM or speed of a processor often measures success in the lithography industry. However, there are scientists and engineers who work diligently behind the scenes on lasers, resists, and optics to make it all happen. The authors would like to thank Dr. R. Akins, Dr. W. Partlo, Dr. I. Fomenkov, Dr. A. Ershov, Dr. V. Fleurov, Dr. G. G. Padmabandu, Dr. P. Zambon, Dr. T. Hofmann, Dr. W. Gillespie, and Dr. M. Purohit for their tireless work in advancing the state of the art of excimer lasers and providing valuable data for this publication. They are some of the unsung heroes of the microelectronics explosion.

References

[1] C. Smith and L. A. Moore, "Fused Silica for 157 nm transmittance," *Proc. SPIE*, vol. 3676, pp. 834–841, Mar. 1999.
[2] H. Levinson, *Principles of Lithography*. Bellingham, WA: SPIE, 2001, ch. 5, pp. 160–165.
[3] P. Das and U. Sengupta, "Krypton fluoride excimer laser," in *Microlithography Science and Technology*, J. Sheats and B. Smith, Eds. New York: Marcel Dekker, 1997, ch. 4, pp. 304–306.
[4] B. Smith, "Optics for photolithography," in *Microlithography Science and Technology*, J. Sheats and B. Smith, Eds. New York: Marcel Dekker, 1997, ch. 3, pp. 263–264.
[5] A. Kroyan, N. Ferrar, J. Bendik, O. Semprez, C. Rowan, and C. Mack, "Modeling the effects of laser bandwidth on lithographic performance," *Proc. SPIE*, vol. 4000, pp. 658–664, Mar. 2000.
[6] H. Levinson, *Principles of Lithography*. Bellingham, WA: SPIE, 2001, ch. 5, p. 159.
[7] W. Oldham and R. Schenker, "193-nm lithographic system lifetimes as limited by UV compaction," *Solid State Technol.*, pp. 95–102, Apr. 1997.
[8] R. Morton, R. Sandstrom, G. Blumentock, Z. Bor, and C. Van Peski, "Behavior of fused silica materials for microlithography irradiated at 193 nm with low-fluence ArF radiation for tens of billions of pulses," *Proc. SPIE*, vol. 4000, pp. 507–510, Mar. 2000.
[9] Y. Ichihara, S. Kawata, I. Hikima, M. Hamatani, Y. Kudoh, and A. Tanimoto, "Illumination system of an excimer laser stepper," *Proc. SPIE*, vol. 1138, pp. 137–143, Jan. 1990.
[10] P. Das and U. Sengupta, "Krypton fluoride excimer laser," in *Microlithography Science and Technology*, J. Sheats and B. Smith, Eds. New York: Marcel Dekker, 1997, ch. 4, pp. 287–290.
[11] W. Partlo, I. Fomenkov, J. Hueber, Z. Bor, E. Onkels, M. Cates, R. Ujazdowski, V. Fleurov, and D. Gaidarenko, "Electric discharge laser with acoustic chirp correction," U.S. Patent 6 317 447 , 2001.
[12] R. Spangler, R. Jacques, D. Brown, J. Algots, and W. Partlo, "Wavelength stabilization in an excimer laser source using piezoelectric active vibration control," *Proc. SPIE*, vol. 4346, pp. 1190–1201, Feb. 2001.

[13] A. Ershov, G. Padmabandu, J. Tyler, and P. Das, "Laser spectrum line shape metrology at 193 nm," in *Proc. SPIE*, vol. 4000, Mar. 2000, pp. 1405–1417.
[14] P. Das and U. Sengupta, "Krypton fluoride excimer laser," in *Microlithography Science and Technology*, J. Sheats and B. Smith, Eds. New York: Marcel Dekker, 1997, ch. 4, pp. 290–294.
[15] W. Partlo, D. Birx, R. Ness, D. Rothweil, P. Melcher, and B. Smith, "High pulse rate pulse power system," U.S. Patent 5 936 988 , 1999.
[16] T. Hofmann, B. Johnson, and P. Das, "Prospects for long pulse operation of ArF lasers for 193 nm microlithography," *Proc. SPIE*, vol. 4000, pp. 511–518, Mar. 2000.
[17] R. Sandstrom, A. Ershov, and V. Fleurov, "MOPA laser architecture for high power laser light sources," in *Proc. SPIE 27th Conf. Microlithography*, Mar. 3–8, 2002.

Palash Das received the Ph.D. degree in physics from Ohio State University.

He has been with Cymer, Inc., San Diego, CA, for 12 years and has been the Vice President of technology development of the company's new business since January 2002. Since joining the company, he has served under various titles in the areas of research, development, and technology, including Principal Scientist on high-power excimer lasers, Program Manager for 1-kHz excimer laser products, and Vice President of Technology. He started his commercial career in 1980 and has worked on numerous gas and solid-state lasers for scientific, industrial, and military applications.

Richard L. Sandstrom received the B.S. degree in physics and the Ph.D. degree in engineering physics from the University of California at San Diego.

He is a Co-Founder of Cymer, Inc., San Diego, CA, and has served as Senior Vice President and Chief Technical Officer since January 1999. Since the company's inception, he has served under various titles in the areas of research, development, and technology, including Vice President of Advanced Research and Vice President of Technology, and has been instrumental in driving Cymer's technology forward.